

# Domain wall mobility, stability and Walker breakdown in magnetic nanowires

<sup>1</sup>A. Mougin, <sup>1</sup>M. Cormier, <sup>1</sup>J.P. Adam, <sup>1,2</sup>P.J. Metaxas, <sup>1</sup>J. Ferré

<sup>1</sup>*Laboratoire de Physique des Solides, Univ. Paris-Sud,  
CNRS, UMR 8502, F-91405 Orsay Cedex, France and*

<sup>2</sup>*School of Physics, MO13, University of Western Australia,  
35 Stirling Highway - Crawley - WA 6009 - Australia*

(Dated: March 23, 2022)

We present an analytical calculation of the velocity of a single  $180^\circ$  domain wall in a magnetic structure with reduced thickness and/or lateral dimension under the combined action of an external applied magnetic field and an electrical current. As for the case of field-induced domain wall propagation in thick films, two motion regimes with different mobilities are obtained, below and far above the so-called Walker field. Additionally, for the case of current induced motion, a Walker-like current density threshold can be defined. When the dimensions of the system become comparable to the domain wall width, the threshold field and current density, stating the wall's internal structure stability, are reduced by the same geometrical demagnetising factor which accounts for the confinement. This points out the fact that the velocity dependence over an extended field/current range and the knowledge of the Walker breakdown are mandatory to draw conclusions about the phenomenological Gilbert damping parameter tuning the magnetisation dynamics.

PACS numbers: 33.55.Fi, 75.70.-i, 42.65.-k, 75.30.Gw

## I. INTRODUCTION

Analysing the behaviour of a magnetic domain wall under the action of an external magnetic field is not a new concept. For example, magnetic bubble memories, in which information was stored in small magnetised areas delimited by domain walls and written by displacement of the walls under magnetic fields, were designed almost 30 years ago [1]. Recently, an alternative approach has been proposed for reversing the magnetisation of a magnetic cell, namely current-induced magnetisation reversal [2, 3]. In this frame, the use of current-induced magnetic domain wall propagation, as suggested by the pioneering work of Berger [3, 4] is nowadays raising a growing interest. Controlling domain wall motion induced by a magnetic field and/or by a current flowing directly into the magnetic element, is thus a main issue in magnetism as well as a technological challenge. Indeed, in the attempt of designing nanowires enabling fast domain wall motion, disperse results have been published so far in regards of the field-induced motion [5, 6, 7, 8, 9] as well as for the current-induced one [10, 11, 12, 13, 14, 15, 16, 17]. Moreover, the tuning of wall damping and motion remains an open problem of magnetisation dynamics.

This article intends to give a global vision of the dependence of domain wall velocity upon magnetic field and current density strengths in nanowires. We analyse the field and current induced propagation, within the framework of previous analytical studies for the viscous regime in thick infinite samples containing a single  $180^\circ$  Bloch domain wall driven by a magnetic field [1, 18, 19]. Indeed, when the effect of the applied magnetic field is sufficient to overcome pinning forces, the wall velocity  $v$  depends linearly on the magnetic field  $H$ , corresponding to viscous motion. Two linear velocity regimes, separated by a complex transient regime, have been predicted to exist, below

and well above a threshold field called the Walker field  $H_W$  [19], delineating the stability of the wall structure. In each linear regime, a relation between the wall mobility  $m = dv/dH$ , the intrinsic Gilbert damping parameter  $\alpha$  [20] and the dynamic domain wall width has been established [18, 19]. There is in the literature a significant dispersion in the interpretation of velocity measurements in nanowires [6, 7, 8, 10], particularly in relation to damping parameters extracted from the latter. This spread, partly addressed in [8], shows how crucial the knowledge of the Walker field is. We demonstrate that the Walker field, calculated for the case of infinite and thick samples containing Bloch walls, is reduced in the case of confined systems. We find also that the same geometry factor affects the Walker-like critical current density which limits the stability regime of the domain wall under current in nanowires.

Up to now, the most widely used magnetic layers and devices rely on domain wall motion in systems with an in-plane magnetic anisotropy [5, 6, 7, 8, 9, 10, 11, 12, 13, 14, 15, 16, 17]. However media with out-of-plane anisotropy are promising candidates for improving the storage density and for designing magnetic logic devices [21]. In this work, perpendicularly magnetised systems will be extensively investigated; however the presence of an in-plane anisotropy will not affect the geometrical parameters relevant for the wall motion outside of the pinning limited regime.

## II. CURRENT AND FIELD INDUCED PROPAGATION OF A BLOCH WALL

We focus on the behaviour of the local magnetisation  $\vec{M}$  inside a domain wall, oriented as defined in Fig. (1a). The length of the out-of-plane magnetised track sketched

in Fig. (1b) is supposed to be infinite, and oriented along  $y$ . One first tries to evaluate the velocity of a wall propagating towards the positive  $y$  values under the action of a magnetic field  $\vec{H}$  applied along the easy axis of magnetisation  $z$  and/or a current density  $\vec{J}_e$  along  $y$ . We focus on structures with a  $180^\circ$  Bloch domain wall.  $\theta(y)$  given in Eq. (1a) stands as a possible wall profile; the wall center is located at  $y_0$  where  $\theta = \frac{\pi}{2}$  and the characteristic domain wall width  $\Delta$  is given in Eq. (1b). Although magnetostatic effects within domain walls are naturally taken into account in numerical work, they are rarely discussed in analytic treatments [22]. In Eq. (1b) and in the following, the demagnetising factors  $N_x$ ,  $N_y$  and  $N_z$  relate to the domain wall itself,  $M_s$  is the saturation magnetisation,  $A$  and  $K_i$  are the exchange and intrinsic anisotropy constants (see methods).

$$\theta(y) = 2 \arctan \left( e^{\frac{y-y_0}{\Delta}} \right) \quad (1a)$$

$$\Delta = \sqrt{\frac{A}{K_i + 2\pi M_s^2 (N_x \cos^2 \varphi + N_y \sin^2 \varphi - N_z)}} \quad (1b)$$

For  $\varphi = 0$  or  $\pi$ , one has an “ideal” Bloch wall with  $\Delta_{\varphi=0} = \sqrt{\frac{A}{K_i + 2\pi M_s^2 (N_x - N_z)}}$ . This expression involves the wall demagnetising factors along those directions in which the system has reduced dimensions:  $N_x$  along the wire width and  $N_z$  through the layer thickness (see methods).

Besides the shape and size of the sample, among the parameters affecting its mobility, the domain wall structure is often neglected in analytic calculations. In particular, for in-plane anisotropy, several wall types may exist depending on the film geometry: C-shaped or Néel like transverse walls in infinite films [23]; Néel-like transverse walls or vortex walls for a narrow wire [24]. The system of coordinates sketched on Fig. (1c) allows one to adapt, via a permutation of the coordinates, the calculations made here for Bloch walls in out-of-plane spin configurations to transverse walls in in-plane spin configurations. Vortex walls, frequently observed in experiments on large nanowires, are not considered in the present article, nor edge effects.

Magnetisation dynamics are described by Eq. (2), in which the precession of the magnetisation proposed by Landau and Lifshitz [25], the dissipative effects introduced by Gilbert [20] and the usually admitted adiabatic and non-adiabatic spin torque terms [26, 27, 28] reflecting the action of current, assuming the geometry of Fig. (1b) are merged together. Discussion on microscopic spin polarised electronic transport is beyond the scope of this paper, in which we just discuss the macroscopic consequences of the presence of the spin-torque terms [26, 27, 28].

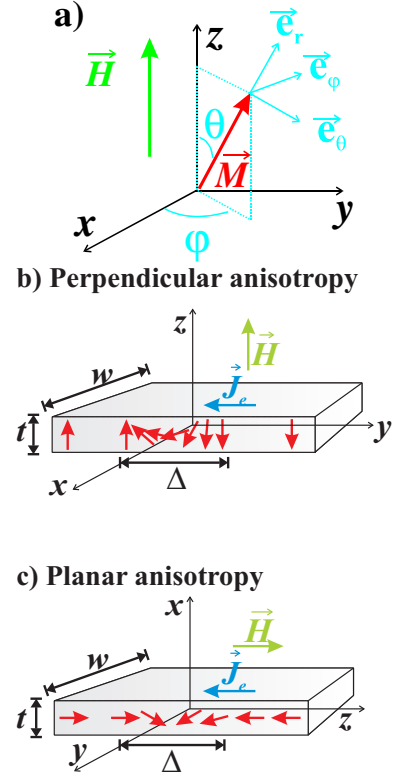


FIG. 1: **a)** Polar  $\theta$  and azimuthal  $\varphi$  angles and the associated spherical coordinate system  $(\vec{e}_r, \vec{e}_\theta, \vec{e}_\varphi)$  defining the orientation of the magnetisation  $\vec{M}$  relative to a Cartesian axis system. **b)** Sketch of a  $180^\circ$  domain wall in a track of width  $w$  and thickness  $t$  showing a perpendicular magnetic anisotropy. **c)** Sketch of the system of coordinates allowing to adapt the calculations to a narrow track with a planar anisotropy.  $\Delta$  denotes the wall width and  $\vec{H}$  the magnetic field applied along  $z$ , defined as the easy magnetisation axis of the magnetic layer in both cases. The current density  $J_e$  along  $y$  is considered as positive if the electrons flow towards the positive  $y$  values.

$$\frac{\partial \vec{M}}{\partial t} = \gamma \vec{H}_{eff} \times \vec{M} + \frac{\alpha}{M_s} \vec{M} \times \frac{\partial \vec{M}}{\partial t} - u \frac{\partial \vec{M}}{\partial y} + \frac{\beta u}{M_s} \vec{M} \times \frac{\partial \vec{M}}{\partial y} \quad (2)$$

In this expression,  $\gamma$  is the gyromagnetic ratio (here a positive quantity) and  $\vec{H}_{eff}$  is the total effective field.  $\beta$  is the phenomenological non-adiabatic spin transfer parameter [26, 27, 28].  $u$  (Eq. 3) has the dimension of a velocity and scales as the electrical current density  $J_e$ :

$$u = \frac{g J_e \mu_B P}{2e M_s} \quad (3)$$

$g$  is the Landé factor,  $\mu_B$  is the Bohr magneton,  $e$  is the electron charge and  $P$  is the polarisation factor of the current.

We express the different torques acting on the magnetisation of the wall region in the  $(\vec{e}_r, \vec{e}_\theta, \vec{e}_\varphi)$  spherical system of coordinates (see methods). From the general kinetic momentum theorem, it is possible to relate the

torque components  $\Gamma_\theta$  and  $\Gamma_\varphi$  and their associated precession velocities  $\dot{\theta}$  and  $\dot{\varphi}$ :

$$\dot{\theta} = \frac{\partial \theta}{\partial t} = -\frac{\gamma}{M_S} \Gamma_\theta \quad (4a)$$

$$\dot{\varphi} = \frac{\partial \varphi}{\partial t} = -\frac{\gamma}{M_S} \Gamma_\varphi \quad (4b)$$

The first torque to be considered (see methods) is that of the external field  $\vec{H}$ , namely  $\vec{\Gamma}_H = \vec{M} \times \vec{H}$  (Eq. 5). The second one  $\vec{\Gamma}_{H_d} = \vec{M} \times \vec{H}_d$  (Eq. 6) is that of the demagnetising field  $\vec{H}_d$  within the wall. The third torque  $\vec{\Gamma}_{H_\alpha} = \vec{M} \times \vec{H}_\alpha$  (Eq. 7) is that of the equivalent damping field  $\frac{-\alpha}{\gamma M_S} \frac{\partial \vec{M}}{\partial t}$ .

$$\vec{\Gamma}_H = \begin{pmatrix} 0 \\ 0 \\ -M_S H \sin \theta \end{pmatrix} \quad (5)$$

$$\vec{\Gamma}_{H_d} = 4\pi M_S^2 \begin{pmatrix} 0 \\ (N_y - N_x) \sin \theta \sin \varphi \cos \varphi \\ \sin \theta \cos \theta [N_z - N_y \sin^2 \varphi - N_x \cos^2 \varphi] \end{pmatrix} \quad (6)$$

$$\vec{\Gamma}_{H_\alpha} = \frac{\alpha M_S}{\gamma} \begin{pmatrix} 0 \\ \dot{\varphi} \sin \theta \\ -\dot{\theta} \end{pmatrix} \quad (7)$$

In the same spirit, assuming that the profile at rest  $\theta(y)$  given in Eq. 1a is conserved under field and/or current, which gives  $\frac{\partial \theta}{\partial y} = \frac{\sin \theta}{\Delta}$ , the adiabatic  $\vec{\Gamma}_u$  and the non-adiabatic  $\vec{\Gamma}_\beta$  spin transfer torques are expressed by Eq. 8 and 9.

$$\vec{\Gamma}_u = \frac{u}{\gamma} \frac{\partial \vec{M}}{\partial \theta} \frac{\partial \theta}{\partial y} = \frac{M_s u \sin \theta}{\gamma \Delta} \vec{e}_\theta \quad (8)$$

$$\vec{\Gamma}_\beta = -\frac{\beta u}{\gamma M_s} \vec{M} \times \frac{\partial \vec{M}}{\partial \theta} \frac{\partial \theta}{\partial y} = -\beta \frac{M_s u \sin \theta}{\gamma \Delta} \vec{e}_\varphi \quad (9)$$

The total polar and azimuthal torques  $\Gamma_\theta$  and  $\Gamma_\varphi$  are given in Eq. 10a and Eq. 10b respectively.

$$\Gamma_\theta = 4\pi M_S^2 (N_y - N_x) \sin \theta \sin \varphi \cos \varphi + \frac{\alpha M_S}{\gamma} \dot{\varphi} \sin \theta + \frac{M_s u \sin \theta}{\gamma \Delta} \quad (10a)$$

$$\Gamma_\varphi = -M_S H \sin \theta - \frac{\alpha M_S}{\gamma} \dot{\theta} - \beta \frac{M_s u \sin \theta}{\gamma \Delta} + 4\pi M_S^2 \sin \theta \cos \theta [N_z - N_y \sin^2 \varphi - N_x \cos^2 \varphi] \quad (10b)$$

### III. WALL VELOCITY AND STABILITY IN SYSTEMS OF REDUCED DIMENSIONS

For a low applied field or current density, in ultra-thin perpendicular magnetised systems, pinning dominates and domain walls move following the creep law [29]. In this non-linear regime, the motion is thermally activated and proceeds by discrete jumps from one pinned configuration to the next. In the following, we assume that pinning effects are overcome and consider only viscous propagation. We first consider the steady domain wall motion, whose signature is a wall moving with a time independent azimuthal angle  $\varphi$ :  $\dot{\varphi} = 0$  which implies that  $\Gamma_\varphi$  (Eq. 10b) must vanish. Writing  $\Gamma_\varphi = 0$  for  $\theta = \pi/2$  (at the wall center where  $\Gamma_\varphi$  has an extremum) gives:

$$\sin 2\varphi = \frac{H + (\beta - \alpha) \frac{u}{\gamma \Delta}}{2\pi \alpha M_s (N_y - N_x)} \quad (11)$$

$$\text{only valid if } \left| H + (\beta - \alpha) \frac{u}{\gamma \Delta} \right| \leq H_W \quad (12)$$

where we define the adapted Walker field by

$$H_W = 2\pi \alpha M_s |N_y - N_x| \quad (13)$$

Eq. 12 sets a limit on the combined strength of the applied field and current density for steady motion to occur.  $\left| H_{ext} + (\beta - \alpha) \frac{u}{\gamma \Delta} \right|$  determines the Walker-like stability condition for the wall motion as a whole. This limit condition is strictly equivalent to the Walker breakdown condition, in the case where only an external magnetic field is applied. Above the Walker breakdown, the stability condition  $\dot{\varphi} = 0$  is broken and the motion is no longer steady. There, the torque of the external field/current dominates those of the demagnetising (Eq. 6) and damping (Eq. 7) fields. It is the  $\varphi$  torque component which fixes the steady regime limit for a wall but the underlying quantity governing the wall's stability is the magnetostatic field inside the wall, making its motion geometry dependant. As a direct illustration, in the steady regime ( $\dot{\varphi}=0$ ) and without current, the only non zero component of the damping torque is the  $\varphi$  component, which is proportional to the rate of change of  $\theta$  and depends only on the demagnetising field. As compared to the expression obtained by Schryer and Walker [19], our expression of  $H_W$  (Eq. 13) includes a geometry factor  $|N_y - N_x|$ . For a zero applied field ( $H = 0$ ) one similarly gets a Walker breakdown current density  $J_W$  (Eq. 14). The same geometrical reduction factor enters the critical Walker-like current density defining the stability condition of the wall.

$$J_W = \frac{4\pi \alpha e M_s^2}{g \mu_B P} \frac{\gamma \Delta}{|\beta - \alpha|} |N_y - N_x| \quad (14)$$

The wall velocity is related to the way the spin aligns along the external field, i.e. to the rate of change of  $\theta$  and

therefore comes out from the resulting torque  $\Gamma_\theta$  given in Eq. 10a. Making use of Eq. 4, in the steady regime ( $\dot{\varphi} = 0$ ),  $\dot{\theta}$  is simply  $-\gamma \times 4\pi M_S(N_y - N_x) \sin \theta \sin \varphi \cos \varphi - u \frac{\sin \theta}{\Delta}$ . The velocity  $v$  of any spin embedded in a Bloch wall is related to the characteristic width by:  $v = -\frac{\Delta}{\sin \theta} \dot{\theta}$ . Choosing again  $\theta = \pi/2$  and using Eq. 11, we obtain:

$$v_{steady} = \frac{\gamma\Delta}{\alpha} \left[ H + (\beta - \alpha) \frac{u}{\gamma\Delta} \right] + u = \frac{\gamma\Delta}{\alpha} \left( H + \frac{\beta u}{\gamma\Delta} \right) \quad (15)$$

This expression is formally equivalent to the one obtained in the Walker theory [19], the magnetic field being here shifted by a spin transfer equivalent field  $\beta u / \gamma \Delta$ . This extra term is linked to the non-adiabatic spin transfer, which is the only spin transfer component efficient for steady motion. As shown for in-plane magnetised samples, the adiabatic component distorts the wall structure but does not induce a stationary motion [26, 28]. It is worth noting that the “ $\beta$  term” does not appear explicitly in the  $\Gamma_\theta$  torque component. It only appears implicitly via its action on the  $\varphi$  precession.

If  $|H + (\beta - \alpha) \frac{u}{\gamma\Delta}| \gg 2\pi\alpha M_S |N_y - N_x|$ , we assume that the precession of the magnetisation occurs at a constant angular speed so that the average value over time of  $\sin 2\varphi(y_0, t)$  can be set to zero. Thus, averaging Eq. 10a and Eq. 10b over a period of the precession of  $\varphi$  and making use of Eq. 4, one gets the average velocity far above the Walker breakdown, simply given by Eq. 16:

$$\bar{v} = \gamma\Delta \frac{\alpha}{1 + \alpha^2} \left( H + \frac{\beta u}{\gamma\Delta} \right) + \frac{u}{1 + \alpha^2} \quad (16)$$

This regime is similar to the usual high field one described for a  $180^\circ$  Bloch wall [1, 18, 19], i.e. the average velocity is linear in the field, following an initial drop in the mobility at the breakdown. The current action is thus i) equivalent to an additional magnetic field  $\beta u / \gamma \Delta$  applied along the anisotropy direction of the system [26, 28] and ii) an extra velocity linked to the adiabatic spin transfer, that is  $u / (1 + \alpha^2)$ , far above the Walker breakdown. Both linear velocity regimes are depicted in Fig. 2, under sole action of a driving field (a) and under the combined action of a field and a current (b).

In a one dimensional statement of wall motion, without current, a qualitative understanding of the damping/demagnetising interrelation is easy to provide. When a drive field is applied along the anisotropy direction,  $\vec{M}$  starts a  $\varphi$  precession movement, and tilts away with respect to its equilibrium orientation at rest, according to the external field torque given in Eq. 5. The out of the  $xz$  wall plane component of the magnetisation creates magnetic charges. The  $\theta$  component of the torque resulting from the induced magnetostatic field (Eq. 6) describes the resulting additional precession of the spin around  $\vec{H}_d$ . Damping and demagnetising torques then rapidly “freeze” the precession by cancelling the Zeeman

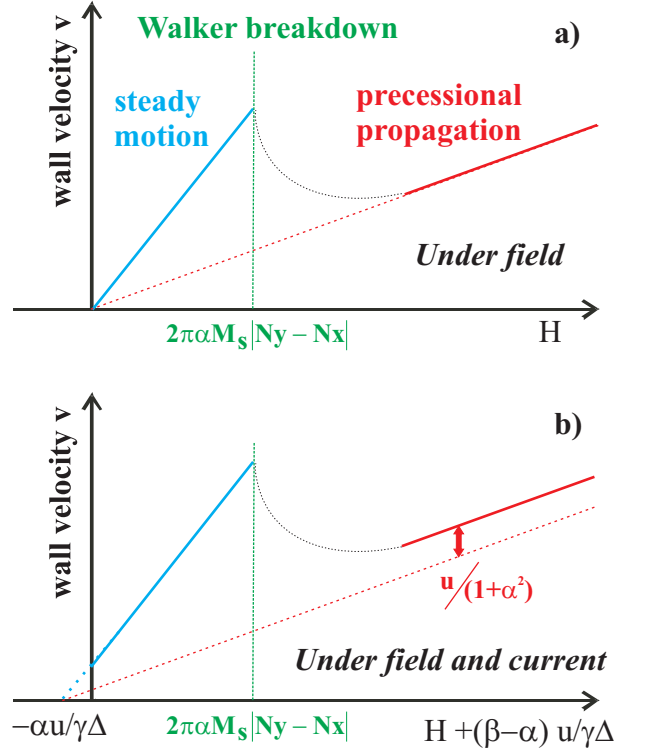


FIG. 2: Sketch of a  $180^\circ$  domain wall's velocity as a function of (a) an external magnetic field  $H$  and (b) a driving term combining a field and a current ( $u$  relates to the current density) in a nanowire. This cartoon indicates the two linear regimes of velocity, below and far above the Walker breakdown. The dotted line in the transient non-linear regime is a guide for the eyes.

torque. At the Walker field, the equilibrium that exists between the damping/demagnetising torque and the drive field torque keeping  $\varphi$  constant is broken and the wall exhibits its maximum velocity for  $\varphi = \pi/4$  in the linear region. Above the Walker breakdown, the azimuthal angle precesses around the external field. The motion is oscillatory, due to the periodic nature of the torque term with respect to  $\varphi$ . In the case where there would be no damping, the wall would move back and forth about its initial position. In the presence of damping, the forward displacement is larger than the backward one. This results in a positive average displacement during one period and hence in a non zero average velocity.

#### IV. DISCUSSION

In contrast to the case of a thick infinite film, one must consider all components of the wall's internal demagnetising field to describe the Walker breakdown of the wall under the action of either a magnetic field or a spin polarised electrical current when the system's dimensions are comparable to, or less than, the domain wall width. For a thick and infinite sample, the only non-zero

wall demagnetising coefficient is the one along  $y$  since the magnetic charges along  $z$  (thickness) and  $x$  (width) are repelled towards infinity (Fig. 3). Said another way, in that geometry, the demagnetising field has only one significant component which is perpendicular to the wall plane and the additional torque related to  $\vec{H}_{dy}$  (through the wall width) is the only one that is efficient in aligning the spin and pushing the wall forward. For a track of reduced dimensions and/or an ultrathin film ( $t \ll \Delta$ ,  $w \ll \Delta$ ), the coefficients  $N_x$  and  $N_z$  are not zero anymore and reflect the aspect ratio  $w/\Delta$  and  $t/\Delta$  (Fig. 3). Since  $N_x + N_y + N_z = 1$ , the demagnetising field  $\vec{H}_{dy}$  perpendicular to the wall and its associated torque will be reduced with respect to the infinite thick film case. Time resolved Kerr microscopy experiments performed on continuous Pt (4.5 nm) / Co ( $0.4 \text{ nm} < t < 0.9 \text{ nm}$ ) / Pt (3.5 nm) layers grown by sputtering with a perpendicular to the plane magnetic anisotropy support the present conclusions [30]. In the case of a nanowire of width  $w=200 \text{ nm}$  patterned from such a Pt(4.5nm)/Co (0.5 nm)/Pt(3.5nm) film, we model the 1D wall cross-section as an ellipse which allows use of the standard expression  $N_y \simeq t/(t + \Delta)$  and  $N_x \simeq t/(t + w)$  [31]. This leads to  $N_x \simeq 0.0025$ ,  $N_y \simeq 0.0775$  and  $N_z \simeq 0.92$ . The Walker threshold field  $H_W$  of the nanowire is then about 7.5% of that of the corresponding thick and infinite layer.

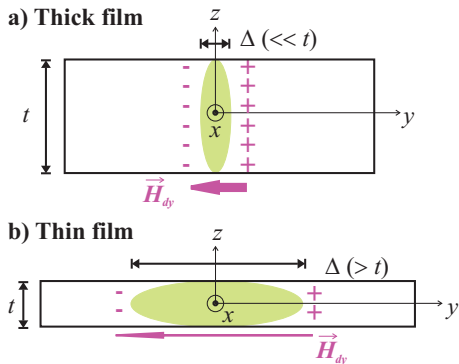


FIG. 3: Sketch of the  $yz$  plane of a  $180^\circ$  domain wall with magnetic charges and the associated  $y$  component of the demagnetising field ( $\vec{H}_{dy}$ ) through the wall plane for different thicknesses.  $\vec{H}_{dy}$  is much smaller in case b) than in case a).

It is in principle possible to evaluate the damping constant  $\alpha$  from domain wall velocity experiments. Under field, this has been tentatively done using in-plane magnetised samples [5, 6, 7, 8] but rarely for out-of-plane magnetised systems [32, 33], in which the creep regime often extends over a large field range [29] and prevents the observation of the linear regimes. The velocity dependence over an extended field/current range and the knowledge of the Walker breakdown are mandatory to draw conclusions about the phenomenological Gilbert damping parameter  $\alpha$ . Experimentally, the first unambiguous evidence of the initial linear regime has been obtained in the case of large area NiFe films (with in-

plane magnetisation) of thickness ranging between 310 and 3000 Å [5]. The authors verified the Bloch nature of the domain wall (above 1000 Å) and then observed an increase of the mobility with the thickness accounted by the domain wall width evolution; for smaller thicknesses and/or samples containing Néel walls, either it was not possible to observe the viscous regime or the thickness dependance was inverse. In the case of a few hundreds Å thick NiFe nanowires of sub-micrometric width,  $v(H)$  experiments have been reported [6, 7, 8, 10]. However, the two successive regimes and the Walker threshold have been evidenced only recently in in-plane systems [8, 10]. For current induced motion, the Walker breakdown was also evidenced recently [11, 12, 16]. Satisfactorily, in [11], the damping constant used to account for the experimental value of the Walker field is compatible with our statement about  $H_W$ .

## V. CONCLUSION

In summary, in the frame of designing devices based on domain wall motion, understanding of the Walker breakdown is critical. Above this breakdown, the wall structure is unstable causing the instantaneous wall velocity to oscillate and the average velocity to drop abruptly. We have demonstrated that wall confinement effects must be taken into account. In nanostructures, magnetostatic effects within the wall lead to a restriction of the stability region relative to thick and infinite films (Eq. 13); the domain wall width parameter  $\Delta$  (Eq. 1b) is also modified. The domain wall structure tuning is also a tricky problem and no consensus has been achieved yet concerning the evaluation of  $\alpha$ . For current induced domain wall motion, dispersed results have been obtained so far, partly because of the distortion of the wall, especially in in-plane systems. Therefore, the choice of perpendicularly magnetised ultrathin layers, whose wall structure is known and in which the non adiabatic contribution should be large [28], are probably good candidates for a detailed understanding of the underlying mechanisms of wall motion and damping as well as for reliability of devices.

## VI. METHODS

### A. Wall's parameters

In the case of a uniformly magnetised ellipsoid, the internal magnetostatic field  $\vec{H}_d$  is proportional to the magnetisation according to  $\vec{H}_d = -4\pi \begin{pmatrix} N_x & 0 & 0 \\ 0 & N_y & 0 \\ 0 & 0 & N_z \end{pmatrix} \vec{M}$ . The demagnetising factors  $N_x$ ,  $N_y$  and  $N_z$  along the  $x$ ,  $y$  and  $z$  directions respectively verify  $N_x + N_y + N_z = 1$ .

Magnetostatic demagnetising factors are complex to calculate in general [1, 34] but they can be evaluated for simple shapes [31, 34].

In the case where an out-of-plane uniform magnetic layer (and not a domain wall) is considered, an effective anisotropy constant is measured:  $K = K_i - 2\pi M_s^2$ , that takes into account the intrinsic anisotropy constant  $K_i$  and the demagnetising field of the out-of-plane saturated layer ( $N_x^{layer} = N_y^{layer} = 0$  and  $N_z^{layer} = 1$ ).

In the case of a pure Bloch wall ( $\varphi = 0$ ), one can compare  $\Delta_{\varphi=0}$  with the domain wall width parameter of a Bloch wall at rest in an infinite and thick layer [19], that is  $\Delta_{Bloch}^{thick} = \sqrt{A/K_i}$ . For an infinite but thin layer, the Bloch domain wall width becomes  $\Delta_{Bloch}^{thin} = \sqrt{A/(K_i - 2\pi M_s^2 N_z)} = \sqrt{A/(K + 2\pi M_s^2 N_y)}$ .

## B. Torque calculations

The torques of the exchange and anisotropy fields compensate each other and therefore are not included in the

torque calculations. They define the wall profile at rest, that is considered as conserved when investigating the dynamics.

The active torques given in Eq. 5, 6 and 7 are obtained using the transfer matrix  $\vec{\Gamma}_{r,\theta,\varphi} = \begin{pmatrix} \sin \theta \cos \varphi & \sin \theta \sin \varphi & \cos \theta \\ \cos \theta \cos \varphi & \cos \theta \sin \varphi & -\sin \theta \\ -\sin \varphi & \cos \varphi & 0 \end{pmatrix} \vec{\Gamma}_{x,y,z}$ .

## Acknowledgments

R.L. Stamps and A. Thiaville are acknowledged for stimulating discussions and a critical reading of the manuscript. J.P.A., J.F. and A.M. acknowledge support by FAST-Egide. Support by the french “ACI PARCOUR” is acknowledged. The stay at Orsay of P.M. is supported by “Marie-Curie Orsay Early Stage Training Site on Emergent Phenomena in Condensed Matter Physics” and FAST. P.M. also acknowledges the Australian Government.

- 
- [1] Malozemoff, A. & Slonczewski, J. *Magnetic domain walls in bubble materials* (Academic Press, New-York, 1979).
  - [2] Slonczewski, J. Current-driven excitation of magnetic multilayers. *J. Magn. Magn. Mater.* **159**, L1–L7 (1996).
  - [3] Salhi, E. & Berger, L. Current-induced displacements of Bloch walls in Ni-Fe films of thickness 120-740 nm. *J. Appl. Phys.* **73**, 6405–6407 (1993).
  - [4] Berger, L. Low-field magnetoresistance and domain drag in ferromagnets. *J. Appl. Phys.* **49**, 2156–2161 (1978).
  - [5] Konishi, S., Yamada, S. & Kusuda, T. Domain-wall velocity, mobility, and mean-free-path in permalloy films. *IEEE Trans. Magn.* **7**, 722–724 (1971).
  - [6] Ono, T. *et al.* Propagation of a magnetic domain wall in a submicrometer magnetic wire. *Science* **284**, 468–470 (1999).
  - [7] Atkinson, D. *et al.* Magnetic domain-wall dynamics in a submicrometer ferromagnetic structure. *Nature Mater.* **2**, 85–87 (2003).
  - [8] Beach, G., Nistor, C., Knutson, C., Tsoi, M. & Erskine, J. Dynamics of field-driven domain-wall propagation in ferromagnetic nanowires. *Nature Mater.* **4**, 741–744 (2005).
  - [9] Fukumoto, K. *et al.* Mobility of domain wall motion in the permalloy layer of a spin-valve-like Fe<sub>20</sub>Ni<sub>80</sub>/Cu/Co trilayer. *J. Magn. Magn. Mater.* **293**, 863–871 (2005).
  - [10] Hayashi, M. *et al.* Influence of current on field-driven domain wall motion in permalloy nanowires from time resolved measurements of anisotropic magnetoresistance. *Phys. Rev. Lett.* **96**, 197207 (2006).
  - [11] Hayashi, M., Thomas, L., Rettner, C., Moriya, R. & Parkin, S. S. P. Direct observation of the coherent precession of magnetic domain walls propagating along permalloy nanowires. *Nat. Phys.* **3**, 21–26 (2007).
  - [12] Beach, G. S. D., Knutson, C., Nistor, C., Tsoi, M. & Erskine, J. L. Nonlinear domain-wall velocity enhancement by spin-polarized electric current. *Phys. Rev. Lett.* **97**, 057203 (2006).
  - [13] Kläui, M. *et al.* Direct observation of domain-wall configurations transformed by spin currents. *Phys. Rev. Lett.* **95**, 026601 (2005).
  - [14] Grollier, J. *et al.* Switching a spin valve back and forth by current induced domain wall motion. *Appl. Phys. Lett.* **83**, 509–511 (2003).
  - [15] Yamaguchi, A. *et al.* Real-space observation of current-driven domain wall motion in submicron magnetic nanowires. *Phys. Rev. Lett.* **92**, 077205 (2004).
  - [16] Thomas, L. *et al.* Oscillatory dependence of current induced magnetic domain wall motion on current pulse length. *Nature* **443**, 197–200 (2006).
  - [17] Vernier, N., Allwood, D. A., Atkinson, D., Cooke, M. D. & Cowburn, R. P. Domain wall propagation in magnetic nanowires by spin-polarized current injection. *Europhys. Lett.* **65**, 526–532 (2004).
  - [18] Slonczewski, J. Dynamics of magnetic domain walls. *Int. J. Magn.* **2**, 85–97 (1972).
  - [19] Schryer, N. & Walker, L. The motion of 180° domain walls in uniform dc magnetic fields. *J. Appl. Phys.* **45**, 5406–5421 (1974).
  - [20] Gilbert, T. *Phys. Rev.* **100**, 1243 (1955).
  - [21] Ravelosona, D. *et al.* Domain wall creation in nanostructures driven by a spin-polarized current. *Phys. Rev. Lett.* **96**, 186604 (2006).
  - [22] D.G. Porter & Donahue, M. Velocity of transverse domain wall motion along thin, narrow strips. *J. Appl. Phys.* **95**, 6729–6731 (2004).
  - [23] Trunk, T., Redjda, M., Kákay, A., Ruane, M. & Humphrey, F. Domain wall structure in permalloy films with decreasing thickness at the bloch to néel transition. *J. Appl. Phys.* **89**, 7606–7608 (2001).
  - [24] McMichael, R. & Donahue, M. Head to head domain wall structures in thin magnetic strips. *IEEE Trans. Magn.* **33**, 4167–4169 (1997).

- [25] Landau, L. & Lifshitz, E. *Physic A Sowjetunion* **8**, 153 (1935).
- [26] Thiaville, A., Nakatani, Y., Miltat, J. & Suzuki, Y. Micromagnetic understanding of current-driven domain wall motion in patterned nanowires. *Europhys. Lett.* **69**, 990–996 (2005).
- [27] Zhang, S. & Li, Z. Roles of nonequilibrium conduction electrons on the magnetization dynamics of ferromagnets. *Phys. Rev. Lett.* **93**, 127204 (2004).
- [28] Tatara, G. & Kohno, H. Theory of current-driven domain wall motion: Spin transfer versus momentum transfer. *Phys. Rev. Lett.* **92**, 086601 (2004).
- [29] Lemerle, S. *et al.* Domain wall creep in an ising ultrathin magnetic film. *Phys. Rev. Lett.* **80**, 849–852 (1998).
- [30] Metaxas, P. J. *et al.* Low and high field domain wall motion in ultrathin Pt/Co/Pt films with perpendicular anisotropy. Submitted to *Phys. Rev. Lett.*
- [31] Osborn, J. Demagnetizing factors of the general ellipsoid. *Phys. Rev.* **67**, 351–357 (1945).
- [32] Tarasenko, S., Stankiewicz, A., Tarasenko, V. & Ferré, J. Bloch wall dynamics in ultrathin ferromagnetic films. *J. Magn. Magn. Mater.* **189**, 19–24 (1998).
- [33] Kirilyuk, A., Ferré, J. & Renard, D. Domain walls in ultrathin ferromagnetic films: velocity and fractal dimension. *Europhys. Lett.* **24**, 403–408 (1993).
- [34] Aharoni, A. Demagnetizing factors for rectangular ferromagnetic prisms. *J. Appl. Phys.* **83**, 3432–3434 (1998).